J. Soc. Cosmet. Scientists Korea
Vol. 36, No. 2, June 2010, 105-113

에토좀 입자크기와 멤브레인 특성 조절을 통한 약물의 경피흡수능 향상

안 은 정*,† · 심 종 원* · 최 장 원*,** · 김 진 웅* · 박 원 석* · 김 한 곤* · 박 기 동** · 한 성 식***

*아모레 퍼시픽 기술연구원, **아주대학교 분자과학기술학과, ***고려대학교 생명과학대학
(2010년 6월 15일 접수, 2010년 6월 20일 수정, 2010년 6월 22일 채택)

Enhanced Transdermal Delivery of Drug Compounds Using Scalable and Deformable Ethosomes

Eun Jung An*,†, Jongwon Shim*, Jang Won Choi*,**, Jin-Woong Kim*, Won Seok Park*, Han-Kon Kim*, Ki-Dong Park**, and Sung-Sik Han***

*Amore-Pacific Co. R&D Center, 314-1, Bora-Dong, Giheung-Gu, Yongin, Gyeonggi-Do 446-729, Korea
**Department of Molecular Science and Technology, Ajou University
***Division of Life Science, College of Life Science and Biotechnology, Korea University
(Received June 15, 2010; Revised June 20, 2010; Accepted June 22, 2010)

요 약: 본 연구에서는 입자 크기 뿐만 아니라 베지클 멤브레인의 변형도를 조절할 수 있는 에토좀을 통해 약물의 경피흡수능을 향상시킬 수 있는 새로운 접근을 소개한다. 이를 위해 신규 육모효능성분인 Triaminodil을 포집한 에토좀을 제조하였고 입자 제조 후 추가적인 에너지를 가함으로써 입자의 크기를 조절하였다. 광산란법, 투과전자현미경, 멤브레인 변형도 측정 등을 통해 입자의 변형도가 입자 크기에 의존하는 것을 확인하였다. 또한 *in vitro* 피부흡수시험과 전임상 성장기 유도평가를 통해 베지클 멤브레인의 변형도가 Triaminodil의 피부 전달효능에 크게 영향을 미치는 것을 확인하였다. 이러한 결과로부터 담지 된 약물의 전달효능을 극대화 시킬 수 있는 최적 크기의 전달체 영역이 존재함을 확인하였고 이는 입자의 크기와 멤브레인 특성에 큰 영향을 받기 때문에 전달체를 설계하는데 있어 이 두 가지 요인을 고려해야 한다.

Abstract: This study introduces a flexible approach to enhance skin permeation by using ethosomes with deformable lipid membranes as well as controllable sizes. To demonstrate this, a set of ethosomes encapsulating an anti-hair loss ingredient, Triaminodil™, as a model drug, were fabricated with varying their size, which was achieved by solely applying the different level of mechanical energy, while maintaining their chemical composition. After characterization of the ethosomes with dynamic light scattering, transmission electron microscopy, and deformability measurements, it was found that their membrane deformability depended on the particle size. Moreover, studies on *in vitro* skin permeation and murine anagen induction allowed us to figure out that the membrane deformability of ethosomes essentially affects delivery efficiency of Triaminodil™ through the skin. It was noticeable in our study that there existed an optimum particle size that can not only maximize the delivery of the drug through the skin, but also increase its actual dermatological activity. These findings offer a useful basis for understanding how ethosomes should be designed to improve delivery efficiency of encapsulated drugs therein in the aspects of changing their length scales and membrane properties.

Keywords: *ethosomes, particle size, deformability, skin permeation, anti-hair loss ingredient*

† 주 저자 (e-mail: ejan@amorepacific.com)

1. Introduction

Stratum corneum, an outermost layer in the skin, is composed of keratin filled corneocytes that are embedded in a lipid enriched intercellular matrix. Its fundamental function is to protect the skin by regulating water loss from inside and by blocking penetration of environmental toxins from outside. The barrier functions of stratum corneum are basically coming from its unique structure[1]. To obtain a more advanced delivery system, it is truly important to understand how stratum corneum is structured and plays its intrinsic functions. For this, physical properties of stratum corneum have been regulated by treating it with chemical enhancers or applying external stresses[2-4]. Also, there has been much effort to develop unique carrier materials that enable better penetration of encapsulated drugs. For examples, a number of techniques have been proposed to disrupt or fluidize the highly organized intercellular lipid matrix, thus enhancing the penetration of the drugs[5].

Since the first report of Meizei et al on the effectiveness of liposomes for skin delivery, use of liposome system has provided many possibilities for increasing the penetration of the drugs through the skin; primarily, deposition of drugs to the skin depends on the lipid composition, lamellarity of liposomes as well as their surface charge[6,7]. However, it is still controversial how liposomes help the drug penetrate the skin layer. It could be either the intact liposomes may directly penetrate into the stratum corneum or the lipid components forming them mix or fuse with the intercellular lipid phase. The former was supported by visualizing the intact liposomes in the dermis layer by using the electron microscope[8]. Further studies also demonstrated that unilamellar vesicles with smaller particle sizes showed the better ability to permeate into the deeper skin strata, compared with larger multi-lamellar vesicles. This supports the idea that the size of liposomes affects the level of their skin deposition[9,10]. Contrary to these studies, however, other studies reported that there could be an optimum particle size leading to more improved skin deposition, implying that the intact liposomes may not penetrate the skin[11,12].

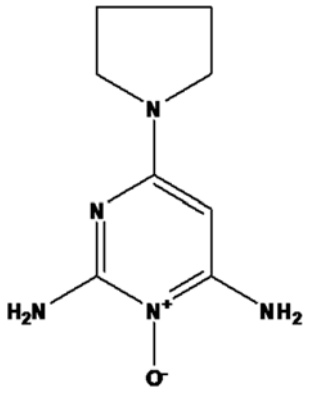

Scheme 1. A molecular scheme of Triaminodil^{TM}.

In most cases, conventional liposomes rather remain confined to the upper layer of the stratum corneum, since they usually have a robust membrane structure. Then, it is essential to provide the liposomes with deformability to enhance dermal and transdermal delivery [7,13]. Deformable liposomal membranes may be achieved either by taking their fusogenic characteristic [14] or by incorporating destabilizing materials, such as surfactants[15,16] and ethanolic components[17,18]. Ethosome is a unique lipid carrier system containing a high concentration of ethanol, developed by Touitou et al.[19]. Although further studies should be carried out to clarify how ethosomes work on enhancing the skin permeation, the synergetic effect coming from chemical enhancing of ethanol and flexible membrane characteristics is known to be responsible for it. Basically, fine control over several key parameters, such as the concentration of ethanol and the type of lipids enables manipulation of particle size, entrapment efficiency of drugs, and flexibility of membrane[20-23].

In this study, we fabricate a representative set of ethosomes that have different deformability, which is done by simply changing their particle size. Our ethosomes can not only solubilize insoluble active drugs in their core or lipid bilayers, but also improve the delivery efficiency through the skin. 4-pyrrolidine 2, 6-diaminopyrimidine-1-oxide, Triaminodil^{TM} (TAD) was chosen as a model drug and evaluate their hair straightening effect (see Scheme 1). TAD opens potassium channels and promotes proliferation of dermal papillae cells that

regulate the hair growing cycle[24-26]. However, this molecule is readily crystallized to form aggregates and causes discoloration or odor variation of formulations, due to its low solubility in both oil and water. From the standpoint of performance and applicability, there is a need for methods to fabricate carriers that can stabilize TAD and promote its dermal delivery. In this study, by using the ethosomes having controllable size and deformability, we try to demonstrate that they are indeed useful for enhancing the transport of TAD, which is characterized by using *in vitro* skin permeation study.

2. Experimental Details

2.1. Fabrication of Size-Controlled Ethosomes

A master sample of ethosomes containing 0.5 wt% Triaminodil (TAD, Proderma, Italy) was prepared by using the method reported by Touitou. Briefly, soybean phosphatidylcholine (Phospholipon 90G, 〉 94 % PC, Lipoid GmbH, Germany) and TAD were first dissolved in a pure ethanol at 30 ℃. Then, double distilled deionized water was slowly added to the solution while mixing with a mechanical stirrer at speed of 700 rpm in a well-sealed glass container. Mixing was carried out for an additional 5 min. The concentrations of TAD, soybean phosphatidylcholine, and ethanol in the ethosomes suspension were set to 0.5, 2, and 30 %. To downnsize the ethosome particle, 200 mL of the solution was taken from the master ethosome sample and homogenized at 6,000 rpm for 5 min at room temperature. The smallest ethosomes were prepared by homogenizing the master ethosome sample (200 mL) with a high pressure homogenizer (Microfluidics, USA) at 600 bar for 3 cycles.

2.2. Characterization of Ethosomes

The size and zeta potential values of ethosomes were determined by using a dynamic light scattering method (Malvern Zetasizer). To measure them, the test suspension was diluted by adding the ethanol solution that had the same ethanol content as the ethosomal suspension[19]. Cryo-TEM was used to investigate the morphology of ethosomes and to directly compare their sizes. For this, the ethosomal suspensions were loaded onto holey-carbon film-supported grids. Then, a thin aqueous film was produced by blotting with a filter paper. The grids were immediately plunged into a liquid ethane before the thin samples began to evaporate. The frozen grids were stored in liquid nitrogen and transferred to a cryotransfer (GATAN model 630, Gatan) under liquid nitrogen. Cryo-TEM (Tecnai-12, Philips) images were then obtained with an accelerating voltage of 120 kV.

2.3. Efficiency of Entrapment

The entrapment efficiency of TAD in ethosomes was determined by dialysis[21]. For this, a regenerated cellulose membrane with a molecular weight cut off of 10,000 (Spectrum laboratories Inc., USA) was kept into a saline solution for 1 h before dialysis to ensure the whole wetting of the membrane ; 2 mL of the ethosome was placed into the dialysis bag, which was then transferred into 500 mL of a phosphate buffered saline solution (pH 7.4). The receiver solution was continuously stirred by a magnetic bar to eliminate the boundary layer effect in each compartment. The experiment was carried out for 24 h at 32 ℃. With the interval, 1 mL of sample was taken from the receiver solution for HPLC analysis. After sampling, the receiver solution was completely removed and replaced with a fresh PBS solution. The method was repeated at least three times.

2.4. Determination of Membrane Deformability

The deformability of ethosomal membranes was determined by the extrusion method[27]. The ethosomal suspensions were extruded through a polycarbonate filter membrane (Whatman Nuclepore Track-Etched Membranes, pore diameter 50 nm, UK). The extrusion was carried out by using Amicon stirred cell (Millipore model 8050, USA), whose diameter is 44.5 mm, by applying a pressure of 2.5 bar. The flux of vesicles that were extruded in 5 min was measured. Vesicle size and size distribution were measured by dynamic light scattering before and after the filtration. The deformability was calculated using the equation $D = J^*(r_v/r_p)^2$, where

D is the deformability of the vesicle membrane, J is the amount of vesicle suspension extruded during 5 min, r_v is the size of vesicles after filtration, and r_p is the pore size of the filter membrane. Statistical analysis was conducted using one-way ANOVA, and significant differences were accepted when $p < 0.05$.(p is the reference to a region of acceptance)

2.5. *In Vitro* Skin Permeation Study

Albino Hartley guinea pigs were purchased from Orient (China) for in vitro permeation study. Full thickness dorsal skin was excised from Hartley albino guinea pigs after sacrificing the animals. Permeation experiments were carried out for 24 h at 32.5 ℃ with Franz-diffusion cells (Hanson Research, USA). Four donor compartments were prepared and filled with ethosome samples ; (a) $Ethosome_{230}$ (large-sized, 230 nm by diameter), (b) $Ethosome_{100}$ (medium-sized, 100 nm by diameter), (c) $Ethosome_{60}$ (small-sized, 60 nm by diameter), and (d) hydroethanolic solution (30 wt% ethanol) for control. These four samples contained 0.5 wt% TAD. Skins were mounted on Franz diffusion cells with a water jacket. The available diffusion area was set to 1.77 cm^2. 7 mL of sample was non-occlusively applied onto the skin. The receiver compartment was filled with a PBS solution (pH 7.4). The solution was continuously stirred with a magnetic bar. 1 mL of sample was taken from the receptor solution every 2 h for 24 h. After sampling, the receptor solution was completely removed and replaced with a fresh PBS solution. Then, the TAD concentration in the receptor solution was determined with HPLC measurements.

2.6. Analysis of Stratum Corneum

To determine the concentration of TAD in the stratum corneum, the test skin taken from the Franz cell was thoroughly washed with the PBS solution. Then TAD in the stratum corneum was analyzed by employing the tape stripping method; an adhesive tape (Cuderm, USA) was pressed the skin to entirely cover the test area (1.77 cm^2) by using a roller. The stripping procedure was repeated until the stratum corneum was completely removed. Complete removal was confirmed by optical microscopic observation; basically guinea pig skins needed 20-times stripping to remove their stratum corneum. The tapes were sonicated for 1 h in a tube containing 5 mL of 80 % ethanol aqueous solution. Then, the remnant skins were cut into small pieces to determine the amount of TAD in the viable skin. The same process as tape cases was used for it. After centrifuge, the concentration of TAD in the supernatant phase was analyzed by using HPLC. All data were expressed as the mean value and standard deviation. ($n \geq 4$, n is the repeating number of experiment). The evaluation of statistical significance was conducted by a one-way analysis of variance (ANOVA). Statistical significance is expressed as $p < 0.05$.

3. HPLC Assay

For HPLC measurements, the mobile phase of HPLC column was made with water, acetonitrile, and methanol with 0.2 % of sodium ethanesulfonate monohydrate (64/27/9, v/v/v). The flow rate was set to 1.5 mL/min and 10 μL of each solution was injected into the chromatograph. Employed stationary phase was RP 18 (250 × 4 mm ; 5 m). An UV detector was employed at the wavelength of 230 nm. The standard solution was prepared by dissolving TAD in a range of 0.005 ~ 0.2 g/mL.

3.1. Murine Anagen Induction Study

The degree of hair-growing activity induced by anagen phase was measured by using 7 week-old (talogen phase) C57BL/6 mice (Samtako, Korea). The dorsal skin of each mouse was shaved with animal clippers. Then, mice were randomly divided into 6 groups. Each group had 7 mice. Six types of formulations were prepared for animal study; a hydroethanolic solution as a vehicle, 0.5 wt% TAD dissolved in the vehicle solution, $Ethosome_{230}$, $Ethosomes_{100}$, $Ethosome_{60}$, and a commercial ointment containing 2 wt% TAD as a positive control. The test formulation was topically applied to the clipped dorsal area twice a day for 3 week. The dorsal skin was photographed when the test was finished. The grown hair weight was determined by measuring reclipped hairs.

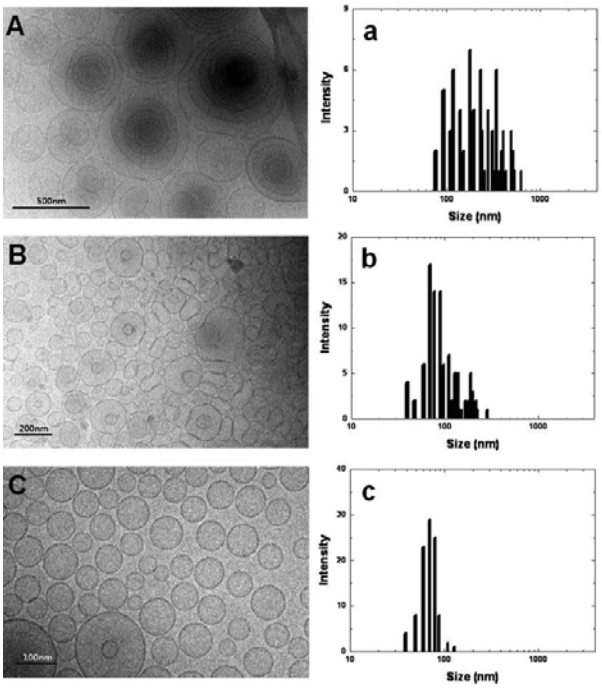

Figure 1. Transmission electron microscope images of the ethosomes down-sized by using different mechanical stirring methods. For this observation, we used a cryo-technique. (A) Ethosome$_{230}$, (B) Ethosomes$_{100}$, and (C) Ethosome$_{60}$. (a) ~ (c) represent the size distributions analyzed with TEM images. The concentration of TAD in the samples was 0.5 wt%.

The evaluation of statistical significance was performed by the two sample t-test. The criterion for statistical significance is expressed as $p < 0.05$.

3.2. Results and Discussion

By regulating the applying level of mechanical energy while making ethosomes, the particle size can be controlled from tens to hundreds of nanometers. A cryo-TEM was used to directly observe the appearance of ethosomes in a suspension state. The result is shown in Figure 1. The TEM images reveals that the length scales and lamellarity of ethosomes are controllable by simply changing the preparation method. The large-sized ethosome particles, Ethosome$_{230}$, were prepared using Touitou's method[19]. They had a multi-lamellar vesicle structure and showed a relatively broad size distribution (Figure 1A). The vesicular membrane of Ethosome$_{230}$ is flexible, since some deformation of the membranes was microscopically observed, when they come closer and packed. The mid-sized ethosome particles, Ethosome$_{100}$, were prepared by homogenizing the master mixture (Figure 1B). Use of homogenization technique decreased the particle diameter-to approximately 100 nm. Ethosome$_{100}$ was still deformable in the process of close packing. The small-sized ethosome particles, Ethosome$_{60}$, were fabricated using a high pressure homogenizer (Figure 1C). The sizes were ~ 60 nm with a narrow size distribution. For Ethosome$_{60}$ sample, any deformation of membranes did not occur during the microscope observation.

The particle size and zeta potential value of the ethosomes were characterized by dynamic light scattering. Results are summarized in Table 1. The mean size was ~ 230 nm, ~ 100 nm, or ~ 60 nm, for Ethosome$_{230}$, Ethosome$_{100}$, and Ethosome$_{60}$, respectively. These sizes were almost consistent with the microscopic sizes determined by TEM measurements. Zeta potential values of the ethosome vesicles had a tendency to decrease slightly with the increase of particle size, but no marked difference was observed. This means that, although the particle size was varied, the surface charge density remained constant, which is likely due to the identical chemical composition. Entrapment efficiency of the ethosomes was not seriously affected by the size variation; TAD was constantly entrapped in the ethosomes by approximately 90 % yield. The long-term storage stability of the ethosomes was observed by measuring the size changes (see Table 2). From the result that there was no significant size increment for several months, it was reasonable to say that the ethosomes prepared in this study had good dispersion stability without any serious coalescence or coagulation, regardless of the particle size. This attributes to the fact that, as reported previously, ethanol has the ability to prevent aggregation of vesicles; due to a net negative surface charge[20].

After phenomenological observation, it seemed that the ethosomes used in this study had different deformability depending on their sizes. To further characterize the ethosomes, the deformability was quantitatively determined using the extrusion method[27]. All ethosomes passed through the pores of the extruder under

Table 1. Physical Characteristics of Ethosomes

Name	Preparation method	Mean diameter (nm)	Polydispersity index	ζ potential (mV)	Entrapment efficiency (%)
$Ethosome_{230}$	Mechanical stirring	229.9	0.50	-25.8 ± 11.1	90.3 ± 2.7
$Ethosome_{100}$	Typical homogenization	102.3	0.18	-20.1 ± 10.8	92.3 ± 0.6
$Ethosome_{60}$	High pressure homogenization	57.6	0.17	-14.6 ± 11.1	89.6 ± 0.3

Table 2. Long-term Storage Stability of Ethosomes

Time	$Ethosome_{230}$		$Ethosome_{100}$		$Ethosome_{60}$	
	Size (nm) / PDI	ζ potential (mV)	Size (nm) / PDI	ζ potential (mV)	Size (nm) / PDI	ζ potential (mV)
0 mon	229.9 / 0.5	-25.8 ± 11.1	102.3 / 0.18	-20.1 ± 10.8	57.6 / 0.17	-14.6 ± 11.1
2 mon	241.0 / 0.48	-24.5 ± 15.7	135.1 / 0.29	-14.5 ± 5.6	42.8 / 0.17	-12.3 ± 4.1
4 mon	255.3 / 0.58	-30.8 ± 6.4	120.3 / 0.122	-15.5 ± 3.6	76.4 / 0.131	-14.4 ± 5.2

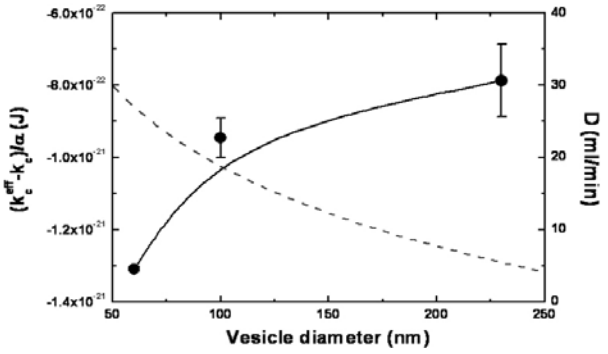

Figure 2. Deformability and effective mean bending modulus of ethosome membranes as a function of vesicle size. The effective mean bending modulus was calculated by using the equation. Here, and were set to 3.210^{-22} and 4.07, respectively [32].

the same pressure, even though the particle size was about 4 times larger than the pore diameter. This suggests that the membrane of the ethosomes was very flexible. This is because ethanol can provide phospholipid bilayers with more fluidity[17]. However, the membrane deformability was reduced as the ethosome size decreased ($p < 0.05$). This can be explained by considering the bending modulus of lipid membranes as a function of vesicle size, as shown in Figure 2. Deformability changes as a function of vesicle size was already characterized in the literatures[28,29]. The size of lipid vesicles is typically determined by competition between curvature energy and entropic terms of the bilayer[30]. In this procedure, the effective mean bending modulus of membrane, k_c^{eff}, at the length scale L of the vesicle size can be expressed by $k_c^{eff}(L) = k_c - \alpha \frac{k_b T}{4\pi} \ln[L/l]$, where k_c is the bending modulus of the membrane and l is a length scale proportional to the size of the molecules[31]. This explains well that smaller vesicles have much higher bending modulus, thus reducing the membrane deformability. Since our ethosomes had the same chemical composition, such reduction of membrane deformability could be associated with the size effect.

The ethosomes used in this study are unique in fact that the deformability and scalability of drug-carrying materials could be correlated with the efficiency of transdermal delivery. This concept was elucidated by directly measuring the delivery efficiency of TAD through skin, as shown in Figure 3. The amount of TAD to be delivered into the receptor compartment was negligible because of its poor solubility in water. Also, although TAD could be dissolved in a hydroenthanolic solution to a certain amount, it was readily crystallized on the skin as ethanol was evaporated; apparently, just an ethanol solution showed the best result, but because TAD is just supersaturated in the ethanol solution. The skin permeation of the ethosomes in the solution state is not accurately comparable with that in an encapsulated state. As can be seen in Figure 3, $Ethosome_{60}$ resulted in the highest level of TAD in the whole skin among all the ethosomes. Taking a closer look at the TAD level in the stratum corneum and the deep skin, however, a different fashion of TAD de-

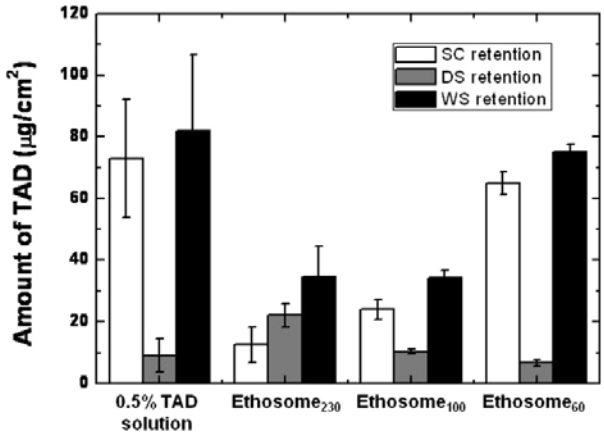

Figure 3. Quantitative analysis of delivery amount of TAD into the skin layers depending on the type of ethosomes. We measured the concentration of TAD in the whole skin (WS), stratum corneum (SC), and deeper skin (DS) of guinea pigs. 0.5 % TAD solution was a control sample, in which TAD was dissolved in a hydroethanolic solution (30 wt% ethanol in water).

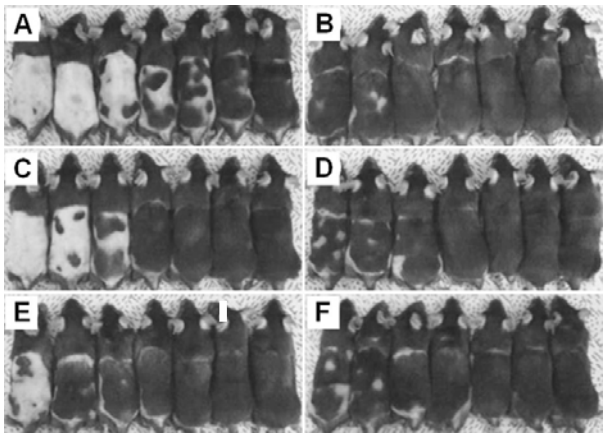

Figure 4. Murine anagen induction by topical administration of TAD. Apparent hair growth for the test animals was observed after every twice treatments of TAD per day for 3 week. (A) vehicle, (B) 0.5 wt% TAD solution, (C) $Ethosome_{230}$, (D) $Ethosomes_{100}$, (E) $Ethosome_{60}$, and (F) ointment containing 2 wt% TAD as a positive control.

livery was observed with respect to the length scale of ethosomes. TAD from $Ethosome_{60}$ was delivered to the stratum corneum by 5-fold higher than that from $Ethosome_{230}$ ($p < 0.05$). By contrast, the analysis for the retention of TAD in the deeper skin clearly showed that $Ethosome_{230}$ had 3.3-fold higher retention amount of TAD than $Ethosome_{60}$ ($p < 0.05$).

In principle, skin permeation of substance is governed by two major factors, which are partition and diffusion [1]. In order to deliver a drug through the skin, either a drug itself or a carrier containing the drug should be partitioned into the upper site of the skin. After this intrinsic process, drug molecules would diffuse into the deeper tissue. In our study, TAD molecules detected after the tape stripping are likely to be the ones that partitioned into the stratum corneum and partially to the hair follicles. It is true that smaller ethosomes have the better ability to contact with the upper site of the skin, since they have larger surface areas as well as higher thermal energy. Differing from this partition case, the diffusion governs delivery of drug molecules in the deeper skin tissue. It has been reported that the deformability of vesicles significantly affect disorganization of the skin barrier, subsequently increasing the skin permeability[7,13,15]. Thus, $Ethosome_{230}$, having the highest deformability, could diffuse more into the deeper skin than other smaller ethosomes. To obtain strong bioavailability, the drug should be delivered into the deeper skin not just to the stratum corneum layer.

To further observe how delivery of TAD via ethosomes works on activating the skin function, *in vivo* skin permeation study was carried out. After topically administrating six TAD formulations to mice for 3 week, hair growth was observed. Apparent hair growth in mice samples is shown in Figure 4. The reclipped hair weight for each test group was also determined and shown in Figure 5. The control group that was treated with hydroetnanolic solution alone showed little hair growth. Whereas, topical application of the ethosomes containing TAD to the clipped dorsal area of telogen phase C57BL/6 mouse significantly helped hairs grow. Among the ethosomes, $Ethosome_{100}$ resulted in the highest hair growth by 36.0 ± 12.0 mg, which was statistically significant ($p = 0.02$). This value was comparable to 0.5 wt% TAD hydroethanolic solution and even to 2 % TAD ointment, the positive control. $Ethosome_{230}$ and $Ethosome_{60}$ showed relatively lower hair growth by 24.0 ± 10.3 and 18.6 ± 8.8 ($p > 0.05$), respectively. These results imply that the ethosome should have an optimum physicochemical property for maximizing the efficiency of transdermal delivery.

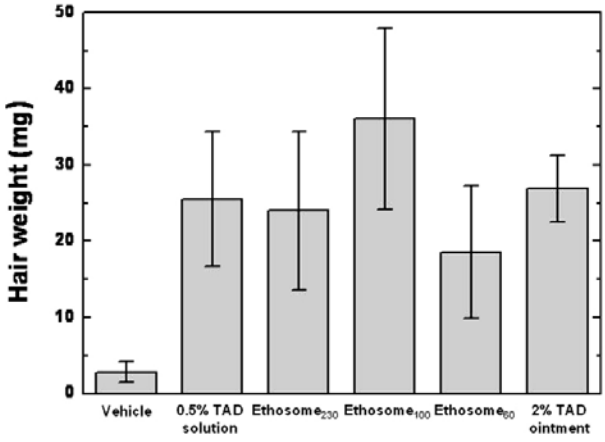

Figure 5. Quantitative analysis of hair growth for test animals. The degree of hair growth was evaluated by measuring the hair weights after treatment of test animals for given time. Treatments of TAD to the test animals was carried out every twice per day for 3 week.

The results obtained from studying *in vitro* skin permeation made two conflicting factors that decide the degree of skin permeability. Smaller ethosomes favorably partition into the stratum corneum but do not have sufficient diffusivity due to the low membrane flexibility. Moreover, they disintegrate easily on the surface of the skin, because they have a unilamellar structure and higher curvature energy[12]. Conversely, larger ethosomes with higher membrane flexibility tend to more penetrate into the deep skin. Unlike *in vitro* skin permeation, the medium-sized ethosomes showed the best hair growth performance in *in vivo* skin permeation. This unique delivery behavior seems to be associated with the difference in the manner of supplying drug molecules. Under *in vitro* condition, drugs are applied in an infinite dose manner, in which a great amount of drugs is continuously supplied to the skin during operation. Under *in vivo* condition, by contrast, no continuous supply of drugs could be made from the donor part. Thus, the window of the optimum ethosome size could be shift to the smaller size, which was ~ 100 nm in our experimental system.

4. Conclusions

This paper experimentally demonstrated that ethosomes could have an optimum size that provides enhanced transdermal delivery of drug compounds. This was possible by fabricating a set of ethosomes with membrane deformability as well as different particle sizes. It was found that smaller ethosomes partitioned easily to the skin. However, they rarely diffused into the deeper skin; due to the rigid membrane property. This suggests that although the smaller vesicles would have the higher diffusion energy, the membrane deformability should also be considered to achieve practical drug efficacy in the skin. *in vivo* skin permeation study showed that an ethosome size could be optimized to -maximize the delivery efficiency. This indicates that the vesicle deformability coming from membrane flexibility should be considered to optimize the length of ethosomes. eventually enabling tuning over both partitioning and diffusion of drug molecules. Taken together, these results provide us with opportunities to design more suitable transdermal delivery carriers with optimized characteristics.

References

1. A. S. Michaels, S. K. Chandrasekaran, and J. E. Shaw, *AIChE J.*, **21**, 985 (1975).
2. M. R. Prausnitz, S. Mitragotri, and R. Langer, *Nat. Rev. Drug Discov.*, **2**, 115 (2004).
3. A. G. Doukas and N. Kollias, *Adv. Drug Deliv. Rev.*, **56**, 559 (2004).
4. A. C. Williams and B. W. Barry, *Adv. Drug Deliv. Rev.*, **56**, 603 (2004).
5. H. A. E. Benson, *Curr. Drug Delivery*, **2**, 23 (2005).
6. M. Mezei and V. Gulasekharam, *Life Sci.*, **26**, 1473 (1980).
7. M. M. A. Elsayed, O. Y. Abdallah, V. F. Naggar, and N. M. Khalafallah, *Int. J. Pharm.*, **332**, 1 (2007).
8. M. Foldvari, A. Gesztes, and M. Mezei, *J. Microencapsul.*, **7**, 479 (1990).
9. R. Natsuki, Y. Morita, S. Osawa, and Y. Takeda, *Biol. Pharm. Bull.*, **19**, 758 (1996).
10. D. D. Verma, S. Verma, G. Blume, and A. Fahr, *Int. J. Pharm.*, **258**, 141 (2003).
11. J. du Plessis, C. Ramachandran, N. Weiner, and D.

G. Mller, *Int. J. Pharm.*, **103**, 277 (1994).
12. M. entjurc, K. Vrhovnik, and J. Kristl, *J Control. Rel.*, **59**, 87 (1999).
13. P. L. Honeywell-Nguyen and J. A. Bouwstra, *Drug Discovery Today : Technologies*, **2**, 67 (2005).
14. M. Kirjavainen, A. Urtti, I. J狎skelinen, T. M. Suhonen, P. Paronen, R. Valjakka-Koskela, J. Kiesvaara, and J. Mnkknen, *Biochim. Biophys. Acta*, **1304**, 179 (1996).
15. G. M. M. El Maghraby, A. C. Williams, and B. W. Barry, *Int. J. Pharm.*, **276**, 143 (2004).
16. M. Trotta, E. Peira, M. E. Carlotti, and M. Gallarate, *Int. J. Pharm.*, **270**, 119 (2004).
17. M. Kirjavainen, A. Urtti, R. Valjakka-Koskela, J. Kiesvaara, and J. Mnkknen, *Eur. J. Pharm. Sci.*, **7**, 279 (1999).
18. N. Dragicevic-Curic, D. Scheglmann, V. Albrecht, and A. Fahr, *Colloid Surf. B : Biointerf.*, **74**, 114 (2009).
19. E. Touitou, N. Dayan, L. Bergelson, B. Godin, and M. Eliaz, *J. Control. Rel.*, **65**, 403 (2000).
20. J. M. Lpez-Pinto, M. L. Gonzlez-Rodrguez, and A. M. Rabasco, *Int. J. Pharm.*, **298**, 1 (2005).
21. D. Paolino, G. Lucania, D. Mardente, F. Alhaique, and M. Fresta, *J. Control. Rel.*, **106**, 99 (2005).
22. S. Jain, A. K. Tiwary, B. Sapra, and N. K. Jain, *AAPS PharmSciTech*, **8**, E1 (2007).
23. Y. P. Fang, Y. H. Tsai, P. C. Wu, and Y. B. Huang, *Int. J. Pharm.*, **356**, 144 (2008).
24. W. S. Park, N. H. Park, J. S. Hwang, and I. S. Jang, The 5th International Congress of Hair Research, Vancouver, Canada (2007).
25. W. S. Park, N. H. Park, J. S. Han, S. Y. Baek, J. S. Hwang, and I. S. Jang, WO patent 046577 (2007).
26. G. C. Davies, M. J. Thornton, T. J. Jenner, Y. J. Chen, J. B. Hansen, R. D. Carr, and V. A. Randall, *J. Invest. Dermatol.*, **124**, 686 (2005).
27. B. A. I. van den Bergh, P. W. Wertz, H. E. Junginger, and J. A. Bouwstra, *Int. J. Pharm.*, **217**, 13 (2001).
28. K. Dimitrievski, *Langmuir*, **26**, 3008 (2010).
29. E. Reimhult, F. H拓k, and B. Kasemo, *J. Chem. Phys.*, **117**, 7401 (2002).
30. M. Antonietti and S. Frster, *Adv. Mater.*, **15**, 1323 (2003).
31. M. M. A. E. Claessens, B. F. van Oort, F. A. M. Leermakers, F. A. Hoekstra, and M. A. Cohen Stuart, *Biophys. J.*, **87**, 3882 (2004).
32. W. Rawicz, K. C. Olbrich, T. Mclntosh, D. Needham, and E. Evans, *Biophys. J.*, **79**, 328 (2000).